2020

Ile126His and Lys129His Surface Mutations Aid in Purification of Haemophilus influenzae Carbonic Anhydrase Through Increased Metal Ion Affinity

Timothy Rigdon
Providence College

Kathleen Cornely
Providence College

Ile126His and Lys129His Surface Mutations Aid in Purification of *Haemophilus influenzae* Carbonic Anhydrase Through Increased Metal Ion Affinity

May 12, 2019

Timothy Rigdon and Kathleen Cornely

From the Department of Chemistry and Biochemistry, Providence College, Providence, RI 02918

Carbonic anhydrase (CA) is an enzyme that plays a major role in the survival of many bacterial, chiefly *Haemophilus influenzae*. Because of its crucial role in bacteria, recent research has turned to CA as a possible target for drug development to kill bacteria and possibly cure different bacterial diseases. While research has focused on this drug target, the isolation and purification of specific types of CA has remained a major obstacle for further research. The current method of immobilized metal affinity chromatography (IMAC) with a Ni-NTA column is used widely for CA purification; however, the *H. influenzae* carbonic anhydrase (HICA) has very low binding affinity to Ni-NTA column and cannot be effectively purified. Previous research has shown that the addition of a surface histidine residue at D125 increases HICA protein binding affinity to the nickel column.

In our research, we suggest that the further insertion of surface histidine residues will increase the HICA protein binding affinity to a Ni-NTA column. The addition of the Ile126His and Lys129His mutations to the Asp125His HICA mutant through site directed mutagenesis is presented here to observe the binding affinity of the mutant HICA to a nickel column, The newly synthesized HICA mutant is reported here to enhance the binding affinity of HICA to the Ni-NTA column, eluting from the column upon addition of between 50 and 100 mM imidazole, as opposed to wild-type HICA protein that elutes upon the addition of 25 mM imidazole. To confirm the presence of the mutant HICA protein in the 50 and 100 mM fractions, SDS-PAGE analysis was used and it is reported here that molecular weight of the monomer of the protein was 19.6 kDa. These promising results indicate that the addition of multiple histidine residues to the HICA enzyme can increase its binding affinity to a Ni-NTA column. As opposed to adding polyhistidine tags to the HICA protein, these results suggest a straightforward strategy to purify the HICA enzyme as well as other proteins for further research in drug development.

Introduction

Carbonic anhydrase (CA) enzymes [EC 4.2.1.1] are a class of enzymes known as zinc metalloenzymes, as they have a Zn^{2+} ion present in their active site. CA is a tetramer and in general is responsible for catalyzing the conversion of carbon dioxide and water to a bicarbonate ion (1):

$$CO_{2(g)} + H_2O_{(l)} \rightleftharpoons H^+_{(aq)} + HCO_3^-{}_{(aq)} \qquad (1)$$

There are three major classes of CA enzymes, α, β, and ɣ CA, which each function similarly in different physiological processes, whether that be maintaining pH balance or CO_2 transport (1). The α-CA was the first class of CA discovered and extensively researched. Found in mammals, this physiological function was confirmed and understood in more detail. At physiological pH, equilibrium between carbon

dioxide and the bicarbonate ion favors the bicarbonate ion. However, the negative charge of the bicarbonate prevents transport across lipid membranes of the cell. To facilitate this transport, CA converts the bicarbonate to carbon dioxide which can then diffuse across the cell. The carbon dioxide can then be converted back to bicarbonate ions if needed through Reaction 1. Due to this conversion for membrane transport, CA aids in maintaining intracellular concentrations of the two molecules, thus being essential for different cellular processes (2).

While the α-CA is found in mammals, the β-CA resides throughout plants and bacteria. Originally discovered in leaf chloroplasts, this β-CA was the first CA identified outside of mammals and while believed to have some role in photosynthesis, was never fully understood (3). In the following years these β-carbonic anhydrases were similarly discovered in the bacteria, *Escherichia coli*. This CA, ECCA [PDB: 1T75], was shown to play a role in bacterial growth and because of that became a target for drug development. Similar to the ECCA enzyme, a β-CA was identified in *Haemophilus influenzae*, a human respiratory tract pathogen that can cause infections such as conjunctivitis and meningitis (4). This carbonic anhydrase, HICA [PDB: 2A8D], plays an important role in pathogen survival as HICA allows for survival in both low and high carbon dioxide environments (4). Because of this important function, as being a β-CA not present in mammals, HICA is a novel target for drug development for infections.

With both ECCA and HICA playing important roles in the survival of bacteria that cause infection in mammals, both enzymes have become the focus for in depth analysis. To analyze the function of these enzymes and develop drugs to inhibit their activity, a process has to be used that can efficiently purify the protein. Commonly, immobilized metal affinity chromatography (IMAC) is used to purify different proteins (5). IMAC functions through the use of transition metal ions such as Ni^{2+}, that are linked to solid resins through chelating ligands such as NTA. To purify the proteins, IMAC capitalizes on the affinity of surface cysteine and histidine residues to the Ni-NTA solid. This optimized IMAC system allows for proteins with an incorporated polyhistidine tag to be isolated easily (5). The issue with this process however, is that polyhistidine tags can affect the native structure of proteins, affecting protein expression and activity (6).

Attempts to purify ECCA without the use of polyhistidine tags in other research using IMAC was surprisingly successful and it was determined to be due to endogenous metal affinity (5). By this, it was determined that histidine clusters located along the surface between dimers, which are solvent exposed, can interact with the two valences on Ni^{2+} of the Ni-NTA column and bind tightly together. The His72, His122, and His160 residues in ECCA all make up this cluster and are found to be between 5 to 7 Å of each other in distance (6). The HICA protein would be expected to act similarly as it shares 38% identity with ECCA; however, HICA does not exhibit this same binding affinity, meaning that these histidine clusters are not present (6). With this in mind, Hoffmann *et al.* hypothesized that mutating surface histidines onto HICA would increase binding affinity to nickel. It was determined that binding affinity did increase after adding a histidine at Arg160. The mutated HICA protein eluted at 190 mM imidazole which was much greater than the wild-type HICA that was reported to have no binding (6). To further this research, Cabral *et al*. mutated HICA to add histidine at the Asp125 residue (7).

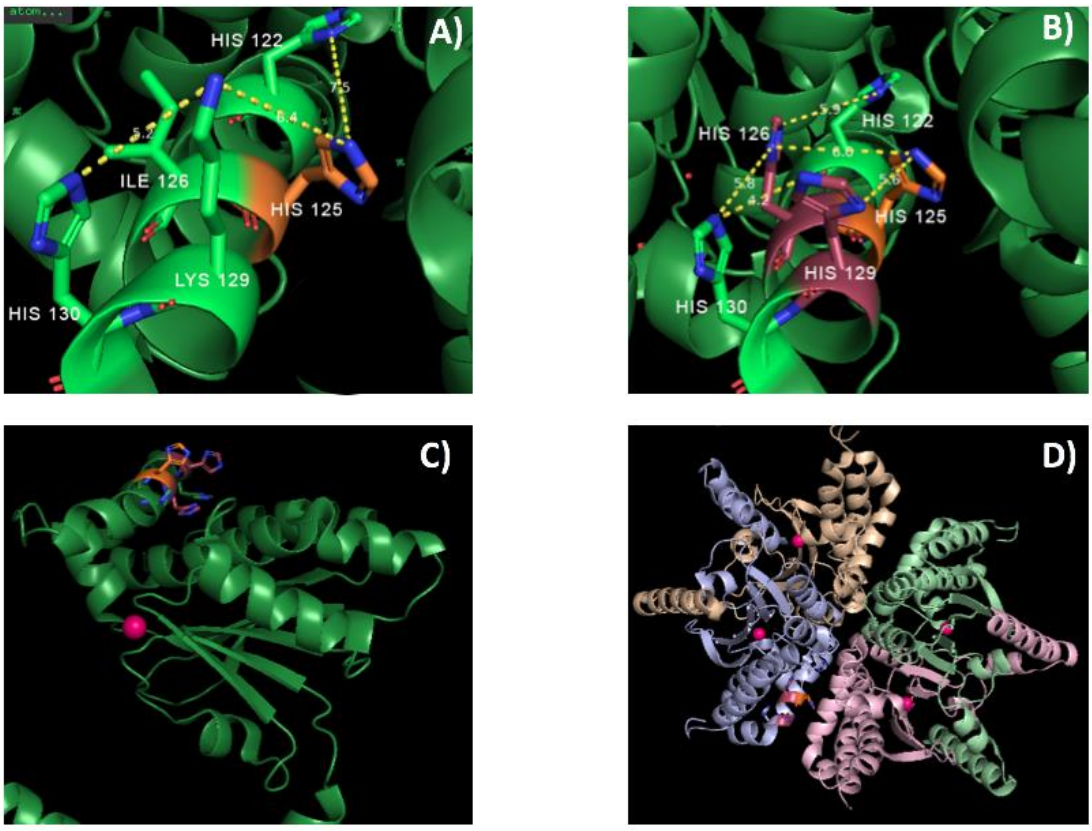

Figure 1. PyMOL generated images of mutated HICA protein. *(A)* This image shows the initial D125H mutated HICA protein [PDB: 2A8D] with neighboring residues on the C monomer. *(B)* This image shows the D125H_I126H_K129H triple mutant HICA protein with neighboring histidine residues on the C monomer. Orange indicates mutations already present. Red indicates novel mutations. *(C)* This image shows the relative distance between the mutated histidine tags and the active site Zn^{2+} ion. The Zn^{2+} ion is indicated by the pink sphere. *(D)* This image shows the homotetrameric structure of the HICA protein with only chains C-F visualized.

They investigated the mutated HICA to determine if there was increased binding affinity with this added histidine residue. This Asp125His is the subject of this work as we look to see the effect on binding affinity of adding additional histidine residues to a previously mutated region of HICA.

Here we report the successful site-directed mutagenesis on the Asp125His mutated HICA protein (7) to further add surface histidines at residues Ile126 and Lys129 following the procedure described by Hoffmann *et al.* (6). With histidine already present at residues 122 and 130, this extended surface of histidine residues created a histidine tag at the surface of the HICA protein that can be visualized in PyMOL Molecular Graphics Service System (Version 2.0 by Schrödinger, LLC). The addition of this tag resembles the binding properties of the ECCA protein and shows increased binding affinity to a Ni-NTA column, needing between 50 and 100 mM imidazole to elute the mutant HICA protein, as opposed to 25 mM imidazole needed for the wild-type protein.

Results

Selection of the Ile126His and Lys129His mutations using PyMOL

To identify possible residues in close proximity to the Asp125His mutation from previous research (7), the HICA protein crystal structure [PDB: 2A8D] was viewed in PyMOL

Molecular Graphics Service System (Version 2.0 by Schrödinger, LLC). Initially the mutagenesis tool was used to insert the Asp125His mutation to the HICA crystal structure on the C monomer (Fig. 1*A*). Then, using the measurement tool the distances between His125, as well as His122 and His130, and surrounding residues were determined to locate possible residues within 5.0 to 7.0 Å of the histidines (6). Ile126 and Lys129 were selected due to their proximity to the three native histidine residues both prior to mutation (Fig. 1*A*) and after mutation (between 4.2 Å and 6.0 Å) with the mutagenesis tool (Fig. 1*B*). With the Ile126His and Lys129His mutations, an extended histidine tag was accessed. Additionally the histidine tag was located on the surface of the protein and distant from the active site (Fig. 1*C*). This ensures proper exposure to the Ni-NTA resin and that the residues mutated are not involved in the catalytic function of the HICA enzyme.

Determination of the presence of Asp125H pHICA in DH5α cells using a restriction digest

To ensure the presence of the HICA gene in the plasmid within the transformed DH5α E. coli cells a series of restriction enzyme digests were performed. The engineered pHICA has restriction sites for the enzymes EcoRV, NcoI, and PstI across the plasmid (Fig. 2). The enzymes were used in the different combinations to ensure the presence of the pHICA from the resultant DNA bands. The digest of NcoI and PstI was expected to produce two DNA fragments at 4132 bp and 695 bp in length. The combination of EcoRV and NcoI was expected to produce two fragments at 4239 bp and 588 bp in length. The digest of PstI and EcoRV was expected to product two fragments at 3544 bp and 1283 bp in length. The final digest using all three enzymes was expected to produce three DNA fragments of the lengths 3544 bp, 695 bp, and 588 bp. These predictions come from the different pHICA restriction sites (Fig. 2). The presence of the correct DNA fragments was confirmed using gel electrophoresis analysis of the digests (Fig. 3). The DNA fragments from the digests verified the presence of pHICA within the transformed DH5α E. coli cells.

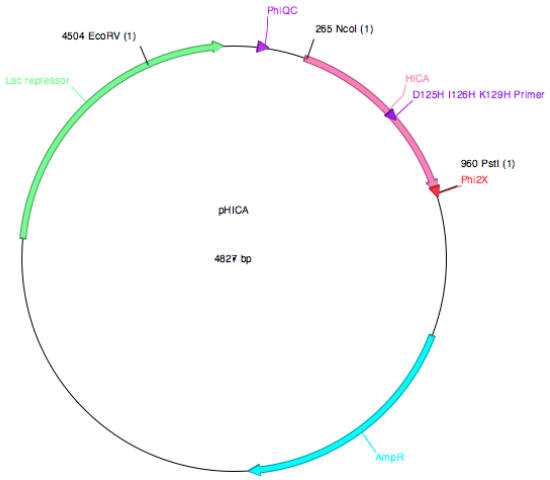

Figure 2. Restriction plasmid map. The map of the pHICA plasmid. The map shows how the plasmid was engineered as well as the PstI, NcoI, and EcoRV restriction sites on the plasmid.

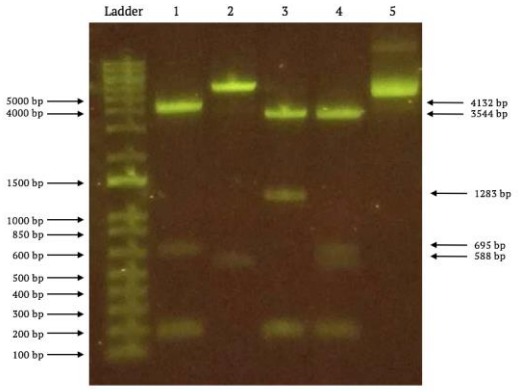

Figure 3. Restriction digest results. This image shows the results of the restriction enzyme digest using the EcoRV, PstI, and NcoI enzymes. Lane 1 shows the NcoI and PstI digest. Lane 2 shows the EcoRV and NcoI digest. Lane 3 shows the PstI and EcoRV digest. Lane 4 shows the digest with all three restriction enzymes. Lane 5 shows the control of the pHICA plasmid DNA with no restriction enzymes.

Table 1

Primers used for site directed mutagenesis of the HICA gene. Mutated histidine residues are indicated in bold. Base changes for histidine mutations are underlined.

Primer	Sequence
Forward Primer (D125H_I126H_K129H)	5'-ATT CGT **CAT CAT** TTG TTT **CAC** CAC GG-3'
Phi2X Reverse Primer	5'-AGC TTG CAT GCC TGC AGT TAT TAT G-3'
PhiQC Forward Primer	5'-CAC TGC ATA ATT CGT GTC GCT CAA GG-3'

Construction of the Ile126His_Lys129His HICA mutant plasmid

With the presence of the Asp125His pHICA confirmed, site directed mutagenesis via megaprimer PCR (8) was performed on the plasmid to generate the Asp125His_Ile126His_Lys129His HICA plasmid in large quantities. The PCR involves three rounds to successfully generate the mutant plasmid, each requiring specificity to ensure addition of the mutations. To ensure the specific binding of the primers to their target sequence (Table 1), a Touchdown PCR protocol was utilized (9). In the first PCR, the two mutations were introduced from the primer (Table 1) with the expected product being 344 bp in length. A band at approximately 344 bp was recovered for use as a primer in the second PCR (Fig. 4).

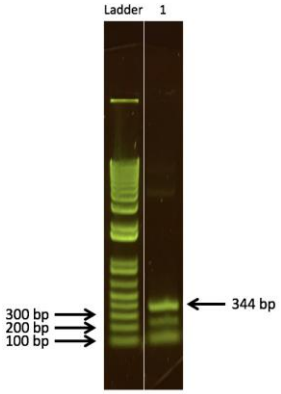

Figure 4. Gel electrophoresis results from the first round of PCR with mutant pHICA. The band at 344 base pairs indicates the successful amplification of the DNA product from the first round of PCR.

In the second PCR, the entirety of the Asp125His_Ile126His_Lys129His HICA was constructed, with the DNA fragment expected to be 883 bp in length. A band approximately at this 883 bp length was obtained and subsequently recovered for use as the megaprimers in the third round of PCR (Fig. 5). The last PCR was expected to amplify the entire Asp125His pHICA of 4827 bp with the Ile126His and Lys129His mutations incorporated. The product from the third PCR was treated with Dpn1 to degrade any of the original Asp125His pHICA DNA. Dpn1 targets methylated DNA for degradation, and the newly synthesized mutant pHICA DNA is not methylated like the original Asp125His pHICA DNA, so the original DNA will be specifically targeted. DNA sequencing was performed on the mutant pHICA in order to confirm the successful addition of the Ile126His and Lys129His mutations via GeneWiz (Cambridge, MA). The sequencing confirmed the success of the site directed mutagenesis in order to generate the Asp125His_Ile126His_Lys129His HICA plasmid.

Overexpression and extraction of Asp125His_Ile126His_Lys129His HICA

To prepare the mutant HICA protein for binding affinity analysis, XJb *E. coli* cells were transformed with the mutant plasmid. The transformed cells were prepared in an overexpression culture with isopropyl βD-1-

thiogalactopyranoside (IPTG), and arabinose. IPTG promotes overexpression of the mutant HICA protein by binding to the lac repression. This allows for the lac operon to bind with RNA polymerase which will transcribe the mutant HICA gene. The cell pellet collected was then lysed to collect the mutant HICA protein by a cycle of freezing and thawing. The added arabinose promoted the expression of λ-lysozyme, which aided in cell lysis by degrading the cell walls. The cells were successfully lysed and then analyzed to determine the protein concentration of lysate.

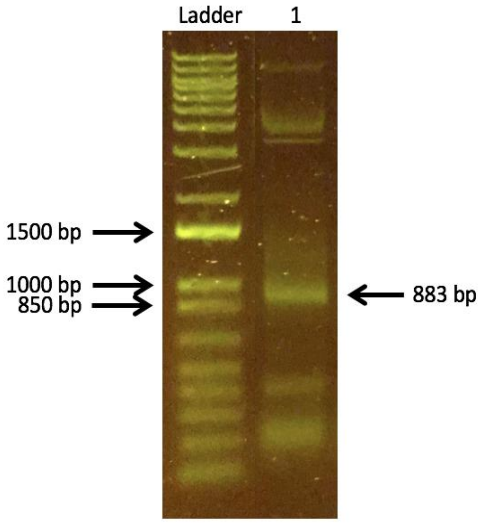

Figure 5. Gel electrophoresis results from the second round of PCR with mutant pHICA. The band at 883 base pairs indicates the successful amplification of the HICA DNA strand from the second round of PCR.

BCA assay on mutant HICA cell lysate

A bicinchoninic (BCA) assay (10) was performed to determine the concentration of the cell lysate. A standard curve was constructed using BCA standard solutions (Fig. 6). The standard curve was used to determine the concentration of the cell lysate of 12.2 ± 0.1 mg/mL.

Ni-NTA chromatography and SDS-PAGE analysis of mutant HICA protein

To determine if the addition of the Ile126His and Lys129His mutations increases the metal affinity of the HICA protein, Ni-NTA chromatography was first performed on the cell lysate. Samples of eluent were captured and absorbance measurements of each eluent fraction were measured at 280 nm, allowing for detection of the mutant HICA protein as it eluted from the column (5). With every wash the concentration of imidazole was increased in order to determine the binding affinity of the mutant HICA protein in relation to imidazole, a known value. The absorbance data from the washes at different concentrations of imidazole were used to construct an elution profile of the mutant HICA protein (Fig. 7*B*). The elution profile shows increased absorbance between the 50 and 100 mM imidazole washes, most likely indicating protein elution from the column. Compared to the elution profile of the wild type HICA protein (Fig. 7*A*) that elutes at 25 mM, the 50-100 mM elution suggests that the mutation results in an increased metal binding affinity.

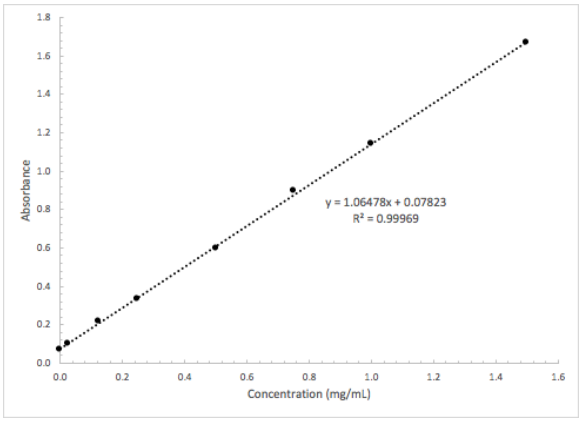

Figure 6. BCA assay for determining mutated HICA protein lysate concentration. The curve from a series of standard solutions of BCA results in a linear relationship between absorbance and concentration. The linear standard curve allows for the determination of the concentration of the mutant HICA protein cell lysate to be 12.2 ± 0.1 mg/mL

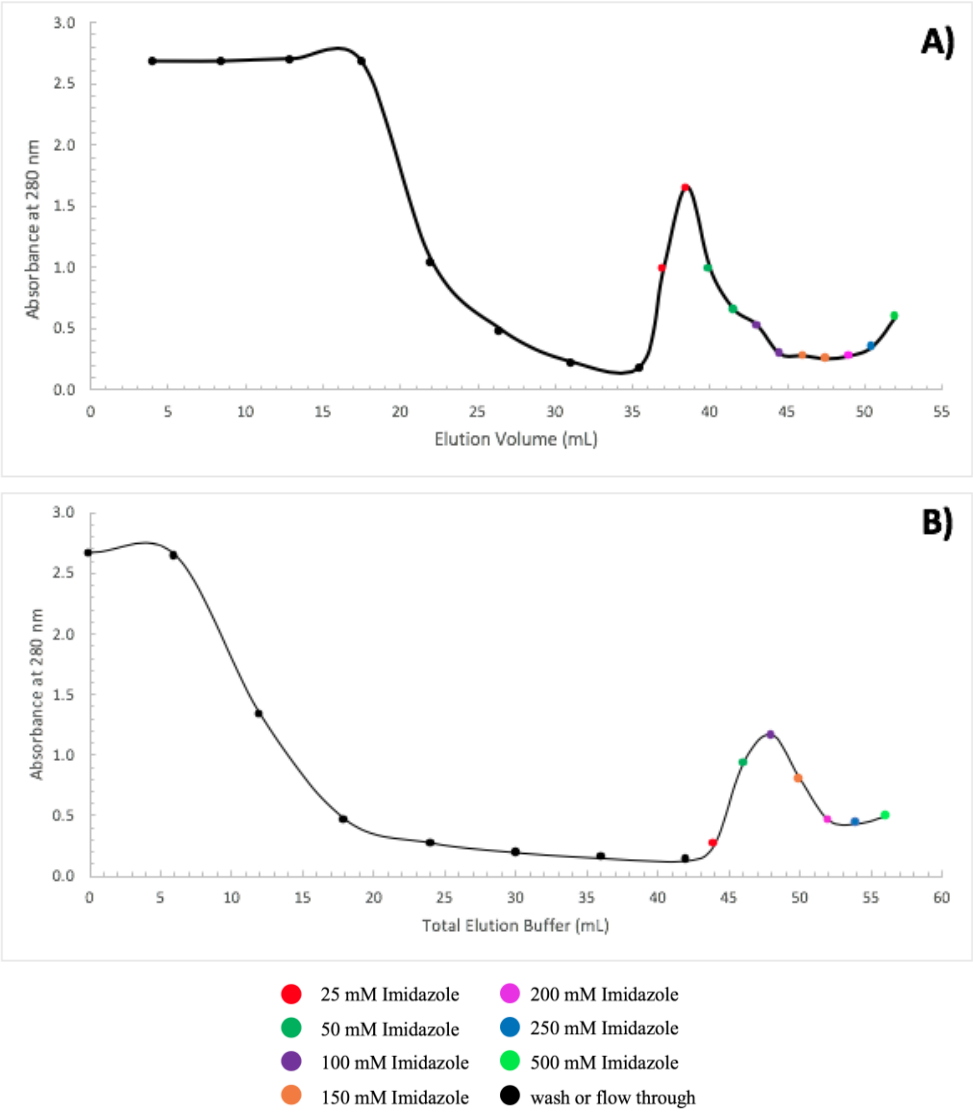

Figure 7. Wild type and mutant HICA protein elution profiles. *(A)* The elution profile for the wild-type HICA protein indicates minimal binding affinity to the Ni-NTA column, with the HICA protein eluting from the column with 25 mM imidazole. *(B)* The elution profile for the D125H_I126H_K129H mutated HICA protein shows that the HICA protein elutes from the column with the addition of 50 mM and 100 mM imidazole.

To confirm that the increased absorbances on the elution profile were due to the elution of the mutant HICA protein, SDS-PAGE analysis was performed on the cell lysate, flow-through, 10 mM imidazole washes, and the 25, 50, 100, and 150 mM elution fractions. Because the samples were treated with SDS and β-mercaptoethanol, the monomer of mutant HICA should be present at 26 kDa. To determine the molecular weight of the protein bands a standard curve of the square root of the molecular weight of the ladder proteins versus the log of the distance each ladder protein band migrated was constructed (Fig. 8*B*). The linear regression of the curve was then used to determine the molecular weight of the protein in the gel bands. The most prominent band, or the one with the darkest blue band, was at 50 mM imidazole (Fig. 8*A*). The calculated molecular weight of the protein at 50 mM imidazole was

19.6 kDa. Though somewhat low, this and the bands at 40 kDa which represent the dimer of HICA, confirm the presence of the mutant HICA protein. There were also faint bands in the cell lysate, 10 mM wash, and the 25 mM, 100 mM, and 150 mM imidazole bands indicating this same molecular weight of 19.6 kDa (Fig. 8*A*).

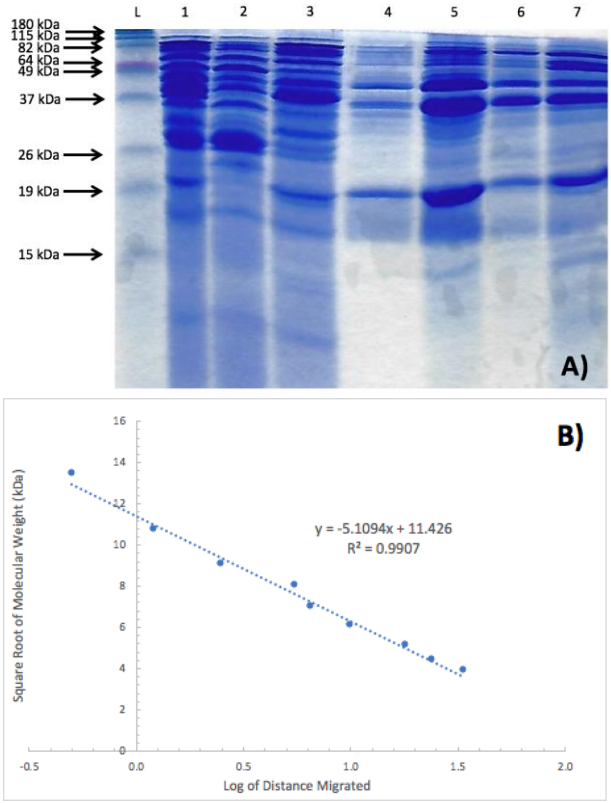

Figure 8. SDS-PAGE analysis of eluent fractions of D125H_I126H_K129H HICA protein. *(A)* The gel from SDS-PAGE indicates the majority of the mutant HICA protein in the 50 mM and 100 mM imidazole fractions. This can be identified by the large, dark blue bands at approximately 19 kDa. The contents of each lane is as follows: (L) ladder, (1) cell lysate, (2) flow through, (3) 10 mM wash fraction, (4) 25 mM imidazole, (5) 50 mM imidazole, (6) 100 mM imidazole, (7) 150 mM imidazole. *(B)* A standard curve of the square root of molecular weight (kDa) v the log of distance migrated of the ladder. The molecular weight of the mutated HICA protein at 50 mM and 100 mM was calculated to be 19.6 kDa.

Discussion

To continue the work of Hoffmann *et al.*, we demonstrate how the addition of surface histidine residues on HICA can aid in its purification by Ni-NTA column chromatography without the need for any polyhistidine tags. Hoffmann *et al.* previously mutated HICA to incorporate a histidine tag present in ECCA in order to increase metal affinity (6). We suggest that independent histidine additions on the surface of the HICA protein can increase metal binding affinity.

The ECCA enzyme has high metal affinity due to the histidine cluster of His72, His122, and His160 on each dimer. This metal affinity leads to concentrations of up to 250 to 300 mM imidazole being required to elute the protein. Within the cluster, the histidine residues between chains are 3.5 to 4.5 Å apart and residues within the same chain are as close as 5 to 7 Å apart (6). The minimal distance between residues allows for optimal nickel coordination as two histidine residues can bind to the two open valences of the nickel resin. While ECCA has high metal affinity, HICA was determined to have minimal natural binding affinity to metals even though HICA has a partially conserved histidine cluster as His160 is replaced by Arg160 (6). To mimic the entire histidine cluster of ECCA, Arg160His was introduced into HICA. It was hypothesized that this mutation would increase HICA's binding affinity. Upon mutation and investigation, Hoffmann *et al.* observed a significant increase in HICA's binding affinity, as when bound to a Ni-NTA column, 190 mM imidazole was needed to elute the mutated HICA protein. While this was still reduced binding as compared to ECCA, the results demonstrated that the metal binding affinity of HICA could be increased through addition of surface histidine residues to the protein (6).

To further the work of Hoffmann *et al.* that concluded adding surface histidine residues could increase HICA's metal binding affinity,

Cabral *et al.* mutated Asp125 to His125 on the HICA protein (7). Asp125 was located on the surface of the HICA protein and was within 7 Å of neighboring histidine residues. Because of the solvent exposure of the residue and proximity to neighboring histidine residues, it was hypothesized that the addition of His125 would increase metal binding affinity to the Ni-NTA column. Upon mutation and investigation, Cabral *et al.* observed a noticeable increase in HICA's binding affinity to the Ni-NTA resin.

To determine viable surface mutations in proximity to the present Asp125His mutation that would increase HICA's metal binding affinity, the crystal structure of HICA was generated in PyMOL Molecular Graphics Service System (Version 2.3 by Schrödinger, LLC). The relative distances between His125, other naturally occurring histidine residues, and other nearby residues were considered when selecting mutations. His125, His122, and His130 were over 7.0 Å apart; however, Ile126 and Lys129 looked to bridge this far separation distance to under 7 Å (Fig. 1*A*). With this in mind, the Ile126His and Lys129His mutations were pursued as they were solvent exposed and had distances of less than 7.0 Å to multiple histidine residues (Fig. 1*B*). The two mutations essentially produced a histidine cluster of five histidine residues: His122, His125, His126, His129, and His130, which could form many different vicinal pairs to bind to the Ni-NTA column. We believed that the addition of the two histidine residues would increase the binding affinity of the HICA enzyme and more closely resemble the ECCA elution profile as opposed to the wild type HICA elution profile.

The Ile126His and Lys129His double mutant was constructed using site-directed mutagenesis of the engineered Asp125His mutated pHICA plasmid (Fig. 2). Results from gel electrophoresis of the first and second round of PCR confirmed the products of proper length were amplified (Fig 4 and 5). Following the construction of the entire mutant plasmid, sequencing by GeneWiz confirmed the successful addition of the Ile126His and Lys129His mutations to the Asp125His pHICA plasmid. The mutated plasmid DNA was transformed into XJb autolysis cells and the mutant HICA protein was overexpressed and then isolated as a cell lysate. The resulting cell lysate was used to examine the mutant HICA's metal binding affinity to a Ni-NTA column. The elution profile constructed from Ni-NTA chromatography suggested that the mutant HICA protein eluted from the column with the addition of 50-100 mM imidazole (Fig. 7*B*).

Following Ni-NTA column chromatography, SDS-PAGE analysis of the collected eluent fractions confirmed the presence of the mutant HICA protein in the 50 mM and 100 mM imidazole fractions, indicated by the dark blue bands at approximately 19 kDa (Fig. 8*A*). The calculated molecular weight of the proteins in the 50 mM and 100 mM imidazole fractions was 19.6 kDa. This corresponds to the HICA protein monomer of 26 kDa. To confirm this, faint bands at approximately 40 kDa indicate the presence of HICA dimer (Fig. 8*A*). The determined molecular weight was lower than expected and this could be due to many possible reasons. It is possible that the protein underwent proteolysis and partially degraded. This would lead to a lower than expected molecular weight however, a protease inhibitor should have reduced these effects. It is also possible that there was aberrant migration caused by increased interactions between SDS and the mutant HICA protein. Increased interaction would lead to more negative charges and an increased migration speed, resulting in a lowered apparent molecular mass. Even so, the confirmation of the presence of the mutant HICA suggests that the addition of multiple surface histidine residues aids HICA purification by increasing metal binding affinity, as Asp125His_Ile126His_Lys129His HICA

required 50 to 100 mM imidazole to elute from the Ni-NTA column.

To detect any binding affinity of wild-type HICA, Ni-NTA chromatography was performed on wild-type HICA as a control and HICA was determined to elute at 25 mM imidazole. These results contradicted those of Hoffmann *et al*. that stated wild-type HICA had no native binding affinity to nickel (6). Even with wild type HICA eluting with 25 mM imidazole, the triple mutant HICA showed stronger binding affinity to the nickel column, eluting with 50-100 mM imidazole. To compare the triple mutant HICA with ECCA's binding affinity, more experimentation should be done to determine the binding affinity of ECCA under the same Ni-NTA conditions. This would allow a more accurate comparison of the difference in binding affinity between the two proteins.

Future experimentation with the Asp125His_Ile126His_Lys129His HICA should look to perform gel filtration in order to confirm the molecular weight of the mutant HICA tetramer. Gel filtration would also help confirm the success of protein overexpression and extraction. Similarly, the gel filtration would give insight to the structural properties of the mutant HICA protein. It is possible that the mutagenesis may have altered the structure of HICA and how HICA coordinates as a tetramer and gel filtration would help to analyze these possibilities.

Along with gel filtration, kinetic experimentation should be performed on the Asp125His_Ile126His_Lys129His HICA in order to analyze the possible effect of the mutations on HICA's enzymatic activity. In the work by Hoffmann *et al*., the Arg160His mutation did not show any alteration in enzymatic activity upon kinetic experimentation (6). The Ile126His and Lys129His mutations were carefully selected according to the guidelines used by Hoffmann *et al*., ensuring that the two mutations were distant from the active site of the enzyme (Fig 1*C*). This suggests that the mutations will have no effect on HICA's enzymatic activity; however, kinetic experimentation would have to be performed to confirm this hypothesis. HICA's catalytic mechanism is reported to involve five residues along the active site: Cys42, Asp44, His98, Cys101, and Gln151, along with a zinc ion (3). The first step of the catalysis of CO_2 to HCO_3^- involves the five active site residues hydrophobically interacting with CO_2. After this, CO_2 is available to be nucleophilically attacked by a zinc bound hydroxide of Asp44. The conversion of CO_2 to a bicarbonate is stabilized by hydrogen bonding with Gln151 on a nearby monomer. Bicarbonate is then released from the active site of HICA, as a water molecule coordinates to the zinc ion to regenerate the ion and Asp44 (3). This putative mechanism does not seem to involve Ile126 and Lys129 so it is expected that the mutation of these residues to histidine should not affect the enzymatic function of the HICA protein. Even so, in depth kinetic analysis should be performed to confirm this.

To this point, we have determined that incorporation of the Ile126His and Lys129His double mutations to the surface of Asp125His HICA leads to the enhancement of the metal ion affinity of HICA. We have confirmed that the triple mutant HICA protein requires 50 to 100 mM imidazole to elute as compared to 25 mM imidazole that is required to elute wild-type HICA. These results expand upon the findings of both Hoffmann *et al*. and Cabral *et al*. by suggesting that enhanced purification can be achieved via IMAC through the addition of surface histidine residues as opposed to a polyhistidine tag. Our results suggest that the addition of multiple histidine residues to create a surface histidine cluster is capable of promoting HICA's metal binding affinity.

Experimental procedures

Bacterial strains and growth conditions

The DH5α *E. coli* strain with the ampicillin resistant pHICA, a plasmid expressing the *H. influenzae* carbonic anhydrase gene, was obtained as a generous gift from Katherine Hoffmann (California Lutheran University, Thousand Oaks, California). The pHICA plasmid was mutated at D125H as described previously (2). The DH5α *E. coli* strain was grown as a liquid culture in a Luria-Bertani medium with 100 mg/mL ampicillin. A liquid culture was made from a frozen stock of the DH5α *E. coli* strain with the ampicillin resistant pHICA plasmid or a single colony was picked from an LB plate containing 3% agar and 100 mg/mL ampicillin which was inoculated into liquid medium and incubated at 37ºC. This plate was streaked from a liquid culture of the DH5α *E. coli* strain from frozen stock. All liquid cultures were incubated at 37ºC for 18 hours.

Plasmid miniprep of DH5α E. coli strain with D125H pHICA

A 1 mL sample of liquid culture of the DH5α *E. coli* strain with the pHICA plasmid with the D125H was purified for the plasmid DNA using a plasmid miniprep kit (Zymo Research). The instructions from the plasmid miniprep kit were followed with the following modifications. In all cases, the centrifuge was operated at 16,000 × g. The pellet from the liquid culture was resuspended using water. After the 50ºC preheated Zyppy Elution buffer, which was composed of 10 mM Tris-HCl, pH 8.5 and 0.1 mM EDTA, was added to the column, the column was allowed to incubate for 20 minutes before centrifuging for 30 seconds. To determine the purity and concentration of the plasmid DNA, the purified plasmid DNA was analyzed using the NanoDrop™ Spectrophotometer (Thermo Fisher).

Restriction enzyme analysis of purified pHICA

Following the plasmid miniprep, enzyme restriction digests were performed in order to confirm the presence of the HICA gene in the plasmid DNA. For the restriction digests, the NcoI, PstI, and EcoRV restriction enzymes were used (New England BioLabs). Four digests were performed with each containing plasmid DNA (176.2 ng). Each digest contained 20 U of the particular enzyme. The first digest included the NcoI and PstI enzymes, the second included the NcoI and EcoRV restriction enzymes, the third included the EcoRV and PstI enzymes, and the fourth restriction digest included all three restriction enzymes. A 1% agarose gel in TAE buffer, composed of 40 mm Tris HCl, 20 mM acetate, and 1 mM EDTA, was executed on the four digests to analyze the products. The results from the digests ensure the inclusion of the HICA gene in the mutant plasmid.

Site directed mutagenesis using PCR

Three rounds of touchdown PCR were completed in order to construct a I126H_K129H mutated pHICA from the original D125H pHICA. The first round of PCR was run to construct a short DNA strand that incorporated the I126H and K129H mutations. The second round of PCR, using the short DNA strand, was run to produce the entire HICA gene with the two mutations. The third round of PCR was run using the mutated HICA gene as a megaprimer to construct the D125H_I126H_K129H mutated pHICA (8).

For the first round of PCR, the primers for the substitutions I126H and K129H were the forward primer 5'-ATTCGT**C**AT**CA**T**T**TTGTTT**CAC**CACGG-3' and the Phi2X reverse primer 5'-AGCTTGCATGCCTGCAGTTATTATG-3' with mutations indicated in bold. All primers were obtained from Integrated DNA Technologies (Coralville, Iowa). Touchdown PCR (9) was carried out using a 25 µL mixture

composed of 88 ng of the D125H mutated pHICA plasmid, 1 µM of the forward primer, 1 µM of the reverse primer (Integrated DNA Technologies), Phusion HF Buffer with 1.5 mM $MgCl_2$ (Thermo Scientific), 200 µM dNTP solution mix (New England BioLabs), and 1 U Phusion High-Fidelity DNA polymerase (Thermo Scientific). The mixture was placed in the thermal cycler with the following program: initial denaturation at 95ºC for 3 minutes, then the following three steps for 30 cycles dropping the annealing temperature by 0.5ºC each cycle; 90ºC for 30 seconds, 60ºC for 30 seconds, 72ºC for 30 seconds. The following three steps were then run for 30 cycles: 95ºC for 30 seconds, 45ºC for 30 seconds, and 72ºC for 30 seconds (11). There was then a final extension of 72 ºC for 7 minutes. A 1% agarose gel was run on the sample at 100V using a TAE electrophoresis buffer in order to separate the sample bands and collect the amplified DNA. Samples were run with a 1 kb Plus DNA ladder and gel loading dye (New England BioLabs). The resulting bands at 344 base pairs were visualized with SYBR Safe DNA gel stain (ThermoFisher) and a transilluminator and then were excised. The gels containing the amplified DNA were then purified according to the instructions from the Zymoclean Gel DNA Recovery Kit (Zymo Research) with the following modifications. DNA elution buffer (10 µL), composed of 10 mM Tris-HCl, pH 8.5 and 0.1mM EDTA, was preheated to 50 ºC and then added to the column matrix and the column was then allowed to incubate for 10 minutes before eluting the DNA.

For the second round of PCR the goal was to amplify the entire HICA gene with the incorporated mutations. The primers used for the second round of PCR were the PhiQC forward primer 5'-CACTGCATAATTCGTGTCGCTCAAGG-3' and the 344 base pair amplified DNA strand from the first round of PCR as the reverse primer. Touchdown PCR was carried out using a 25 µL mixture composed of 88 ng of the D125H mutated pHICA plasmid, 1 µM of the PhiQC forward primer, 6 µL of the reverse primer, Phusion HF Buffer with 1.5 mM $MgCl_2$, 200 µM dNTP solution mix, nuclease free water, and 1 U of Phusion High-Fidelity DNA polymerase. The mixture was placed in the thermal cycler with the following program: 95ºC for 2 minutes, 40 cycles of 95ºC for 30 seconds, 65ºC for 30 seconds, and 72ºC for 1 minute. After each cycle the annealing temperature was decreased by 0.5ºC. After the 40 cycles, there was a 10 minute extension at 72ºC. A 1% agarose gel was run on the sample at 100V using a TAE electrophoresis buffer in order to separate the sample bands and collect the amplified DNA. Samples were run with a 1 kb Plus DNA ladder and gel loading dye. The resulting bands at 883 base pairs were visualized with a transilluminator and excised. The gels containing the amplified DNA were then purified according to the instructions from the Zymoclean Gel DNA Recovery Kit (Zymo Research) with the modifications as described above.

The goal of the third round of PCR was to amplify the entire pHICA plasmid with the incorporated mutations. The primer used for the third round of PCR was the 883 base pair amplified HICA gene from the second round of PCR, acting as the forward and reverse primers. Touchdown PCR was carried out using a 25 µL mixture composed of 88 ng of the D125H mutated pHICA plasmid, 5 µL of the primer, 1.5 mM of Phusion HF Buffer, 200 µM dNTP solution mix, nuclease free water, and 1 U of Phusion High-Fidelity DNA Polymerase. The mixture was placed in the thermal cycler with the following program: 95ºC for 2 minutes, 30 cycles of 95ºC for 1 minute, 65ºC for 1 minute, and 72ºC for 5 minutes. Then there was a 10 minute extension at 72ºC. The resulting product was mixed with 20 U of Dpn I (New England BioLabs). The Dpn I was added to digest the original pHICA plasmid, leaving the mutated pHICA plasmid. The PCR sample was incubated for 2 hours and 45 minutes with DpnI and the

sample was then used for bacterial transformation. The DpnI successfully digested parent plasmids due to methylation that is not present in the mutant plasmid.

Bacterial transformation with DH5α E. coli strain cells

A 2.5 µL sample of the Dpn I-treated mutated pHICA plasmid solution from the third round of PCR was mixed with 50 µL of Zymo DH5α Z-competent *E. coli* cells and allowed to incubate for 60 minutes on ice to allow for the cells to take in the mutated pHICA. After incubation two LB + amp plates were streaked with either 5 µL or 45 µL of the DH5α Z-competent *E. coli* cells and the plates were incubated at 37ºC for 20 hours.

Preparing liquid cultures from DH5α E. coli strain cells with D125H_I126H_K129H pHICA

Colonies from the plates inoculated with the Zymo DH5α Z-competent *E. coli* cells from bacterial transformation were inoculated with LB medium with 100 µg/mL ampicillin to prepare liquid cultures of the DH5α Z-competent *E. coli* cells with the D125H_I126H_K129H pHICA. Liquid cultures were incubated in a roller drum at 37ºC for 19 hours.

Plasmid miniprep of DH5α E. coli strain with D125H_I126H_K129H pHICA

A 1 mL sample of liquid cultures comprised of DH5α Z-competent *E. coli* cells with the pHICA plasmid and the D125H_I126H_K129H mutations that grew for 18 hours at 37ºC were purified for isolation of plasmid DNA using a plasmid miniprep kit with the modifications as described above as well as using TE elution buffer (10 mM, pH 7.5) for elution.

Sequencing of mutant pHICA DNA

The isolated, mutated pHICA DNA was sequenced by GeneWiz (Cambridge, MA). The DNA samples were prepared according to the guidelines given by GeneWiz. Each sample was prepared to a final pHICA DNA concentration of 50 ng/mL in 10 mM Tris. The M13-48REV universal primer was selected for use by GeneWiz. The sequencing results confirmed the successful mutagenesis of the D125H_I126H_K129H pHICA DNA.

Transformation of E. coli Xjb autolysis cells

The transformation of *E. coli* Xjb autolysis cells (Zymo Research) with the D125H_I126H_K129H mutated pHICA was performed following the same procedure as mentioned above for the DH5α cells. After transformation, a colony of the Xjb cells was used to inoculate a 10 mL liquid culture of LB + amp. The culture was allowed to incubate overnight at 37ºC while shaking at 250 rpm.

HICA protein overexpression and cell lysis

The liquid culture of mutated pHICA transformed Xjb cells was pelleted and washed twice with fresh LB medium. The resuspended Xjb cells were then added to 1 L of TerrificBroth (TB) medium (89 mM potassium phosphate, pH 7.2). Arabinose (3.0 mM) was added to the overexpression culture in order to stimulate HICA protein overexpression. Ampicillin (0.1 mg/mL) was added to the mixture. The overexpression culture was incubated at 37ºC with constant shaking at 250 rpm for four hours, until the Xjb cells were in log phase which was determined by the absorbance value of the mixture rising above 0.800 at 600 nm. After this, IPTG (isopropyl β-D-1- thiogalactopyranoside) was added to the mixture to a final concentration of 0.5 mM and the overexpression culture was allowed to incubate overnight at 37ºC with constant shaking at 250 rpm. The next day the cells were harvested by centrifugation 8000 × g for ten minutes. The harvested cells underwent a freeze and thaw cycle at -80ºC to promote lysozyme release and cell wall degradation. After thawing, the cells were resuspended in lysis buffer (20 mM Tris, 100 mM NaCl, pH 8.0) to a

concentration of 3 mL/g and shaken to induce lysis. A protease inhibitor minitablet (Pierce) and 1 mg of lysozyme were then added to the mixture. The solution was then incubated for 20 minutes while shaking at 37ºC. DNAase (1 mg) was then added to the mixture and incubation and shaking was then continued for 17 minutes. The cell lysate was centrifuged for 30 minutes at 35,000 × g. This centrifugation was repeated with the supernatant from the first cycle of centrifugation. The isolated lysate was the dialyzed in a Mega Pur-A-Lyzer (PN: PURG60015, 6-8 kDa MWCO) with PBS (20 mM sodium phosphate, 300 mM NaCl, pH 7.4) for four days. The dialysis was conducted to transfer the lysate to a Tris free buffer, as Tris interferes with protein binding to the Ni-NTA column. The PBS buffer was changed twice with 3 L PBS through the four days to fully dialyze the lysate.

Protein concentration determination with BSA Assay

A BCA Assay (10) was executed to determine the protein concentration of the cell lysate. The assay was performed following the guidelines within the Pierce BCA Protein Assay Kit (ThermoFisher).

Ni-NTA chromatography

Ni-NTA resin (60 mg/mL) was suspended in PBS buffer and the mixture was centrifuged and the buffer was discarded. The cell lysate (120 mg) was added to the Ni-NTA mixture and was mixed on an end-over-end rotator for 60 minutes at 4ºC. The mixture was then added to the column and the flow-through eluent was collected. The resin was washed with three resin bed-volumes of wash buffer, comprised of PBS with 10 mM imidazole, until the wash eluent had an absorbance of less than 0.1 at 280 nm. The bound protein on the Ni-NTA column (6) was eluted with one resin bed-volume of PBS containing 25 mM imidazole. The eluent was collected and the absorbance was measured at 280 nm. This elution process was repeated with PBS containing 50 mM, 100 mM, 150 mM, 200 mM, 250 mM, and 500 mM.

SDS-PAGE

The different eluent fractions from the Ni-NTA column chromatography were used to determine the presence of the D125H_I126H_K129H mutant HICA through SDS-PAGE. The procedure described by Laemmli (12) was followed closely with the following modification: 15% separating gel was used in this project. The samples collected from IMAC with the Ni-NTA column were prepared for use with 1% β-mercaptoethanol and 0.005% bromophenol blue in the solutions. The samples were then denatured at 100ºC for 2 minutes and loaded on to the gel. The loaded gel was run at 55 mamps through the stacking gel and then at 30 mamps through the separating gel for a total of 5 hours. The completed SDS-PAGE gel was then stained a Coomassie Blue staining solution, composed of 0.025% Coomassie Blue R-250, 40% methanol, and 7% acetic acid, for 17 hours. The stained gel was then de-stained for approximately 6 days in a destaining solution composed of 40% methanol, 7% acetic acid, and 3% glycerol. The destaining solution was changed once after 3 days. The destained gel was then dried for 2 hours at 80ºC and 2 hours at room temperature while under vacuum.

Author Contributions—Both authors equally contributed in the completion of this research. Timothy Rigdon performed the described experiments in this research. Dr. Kathleen Cornely provided a detailed outline of the project and executed experiments that were not completed during laboratory hours.

Acknowledgements— We would like to acknowledge Dr. Katherine Hoffmann (Department of Chemistry, California Lutheran

University, Thousand Oaks, California) for her generous gift of DH5α E. coli cells previously transformed with the HICA plasmid. We also acknowledge Jennifer Cabral for her previous work in synthesizing the D125H mutated pHICA used in this research. We acknowledge Robert Lesch for providing us with the restriction enzyme analysis data. We acknowledge Andrew Josling for providing us with the wild-type HICA elution data. We also acknowledge New England BioLabs for their generous donation of reagents for the restriction enzyme analysis. We acknowledge Michelle Thai from Zymo for help with optimizing the plasmid miniprep procedure. We also acknowledge the Providence College Department of Chemistry and Biochemistry for their support and project funding.

References

1. Cronk, J. D., Endrizzi, J. A., Cronk, M. R., O'neill, J. W., & Zhang, K. Y. (2001). Crystal structure of *E. coli* β–carbonic anhydrase, an enzyme with an unusual pH–dependent activity. *Protein Science*. **10**:5, 911-922.
2. Supuran, C. T. (2011) Bacterial carbonic anhydrases as drug targets: toward novel antibiotics? *Front. Pharmacol.* **2**:34, 1-6.
3. Rowlett, R. S. (2010) Structure and catalytic mechanism of the β-carbonic anhydrases. *Biochim. Biophys. Acta.* **1804**, 362-373.
4. Langereis, J. D., Zomer, A., Stunnenberg, H. G., Burghout, P., and Hermans, P. W. M. (2013) Nontypeable *Haemophilus influenzae* carbonic anhydrase is important for environmental and intracellular survival. *J. Bacteriol.* **195**, 2737-2746.
5. Block, H., Maertens, B., Spriestersbach, A., Brinker, N., Kubicek, J., Rabis, R., Labahn, J., and Schäfer, F. (2009) Immobilized- metal affinity chromatography (IMAC): A review. *Methods Enzymol.* **463**, 439-473.
6. Hoffmann, K. M., Wood, K. M., Labrum, A. D., Lee, D. K., Bolinger, I. M., Konis, M. E., Blount, A. G., Prussia, G. A., Schroll, M. M., and Watson, J. M. (2014) Surface histidine mutations for the metal affinity purification of a β-carbonic anhydrase. *Anal. Biochem.* **458**, 66-68.
7. Cabral, Jennifer G. and Cornely, Kathleen, *D125 Surface Histidine Mutation to Gain Metal Affinity of HICA β-Carbonic Anhydrase.* Department of Chemistry and Biochemistry, Providence College, One Cunningham Square, Providence, RI 02918.
8. Barik, S. (1996) Site-directed mutagenesis in vitro by megaprimer PCR. *Methods Mol Biol*. **57**, 203-215.
9. Don, R. H., Cox, P. T., Wainwright, B. J., Baker, K., and Mattick, J. S. (1991) 'Touchdown' PCR to circumvent spurious priming during gene amplification. *Nucleic Acids Res*. **19**, 4008.
10. Smith, P. K., Krohn, R. I., Hermanson, G. T., Mallia, A. K., Gartner, F. H., Provenzano, M. D., Fujimoto, E. K., Goeke, N. M., Olson, B. J., and Klenk, D. C. (1985) Measurement of protein using bicinchoninic acid. *Anal Biochem.* **150**, 78-83.
11. Roux, K. H., and Hecker, K. H. (1997) One-step optimization using touchdown and stepdown PCR. *Methods Mol Biol*. **67**, 39-45.
12. Laemmli, U. K. (1970) Cleavage of structural proteins during the assembly of the head of bacteriophage T4. *Nature*. **227**, 660-685.